

Zirconium-doped lithium niobate: photorefractive and electro-optical properties as a function of dopant concentration

Giovanni Nava,¹ Paolo Minzioni,^{1,*} Wenbo Yan,^{1,2} Jacopo Parravicini,^{1,4}
Daniela Grando,¹ Eleonora Musso,¹ Ilaria Cristiani,¹ Nicola Argiolas,³ Marco Bazzan,³
Maria Vittoria Ciampolillo,³ Annamaria Zaltron,³ Cinzia Sada,⁵ and Vittorio Degiorgio¹

¹Electronics Department and CNISM, University of Pavia, Via Ferrata 1, 27100 Pavia, Italy

²School of Materials Science & Engineering, Hebei University of Technology, Tianjin 300130, China

³Physics Department and CNISM, University of Padova, Via Marzolo 8, 35131 Padova, Italy

⁴Currently with Dipartimento di Ingegneria Elettrica e dell'Informazione, Università de L'Aquila, Via Gronchi 18,
67100 L'Aquila, Italy

*paolo.minzioni@unipv.it

Abstract: Measurements of refractive indices, electro-optic coefficients and photorefractivity are performed for a set of Zirconium-doped congruent lithium niobate (Zr:LN) crystals as functions of the dopant concentration in the range 0.0-3.0 mol%. The photorefractive properties are studied by measuring the green-light induced birefringence change and by direct observation of the transmitted-beam distortion. The index of refraction data show that the threshold concentration, above which there is a change in the Zr incorporation mechanism, is about 2.0 mol%, but photorefractivity results suggest that the concentration of ZrO₂ required to strongly reduce the photorefractive effect is somewhat larger than the 2.0 mol% “threshold” concentration derived from index-of-refraction data. The electro-optic coefficients are little influenced by Zr-doping. All the reported results confirm that Zr:LN is a very promising candidate for the realization of efficient electro-optic and all-optical nonlinear devices working at room temperature.

©2011 Optical Society of America

OCIS codes: (160.5320) Photorefractive materials; (190.0190) Nonlinear optics; (160.3730) Lithium niobate.

References and links

1. L. Razzari, P. Minzioni, I. Cristiani, V. Degiorgio, and E. P. Kokanyan, “Photorefractivity of Hafnium-doped congruent lithium-niobate crystals,” *Appl. Phys. Lett.* **86**(13), 131914 (2005).
2. S. Li, S. Liu, Y. Kong, D. Deng, G. Gao, Y. Li, H. Gao, L. Zhang, Z. Hang, S. Chen, and J. Xu, “The optical damage resistance and absorption spectra of LiNbO₃:Hf crystals,” *J. Phys. Condens. Matter* **18**(13), 3527–3534 (2006).
3. P. Minzioni, I. Cristiani, J. Yu, J. Parravicini, E. P. Kokanyan, and V. Degiorgio, “Linear and nonlinear optical properties of Hafnium-doped lithium-niobate crystals,” *Opt. Express* **15**(21), 14171–14176 (2007).
4. Y. Kong, S. Liu, Y. Zhao, H. Liu, S. Chen, and J. Xu, “Highly optical damage resistant crystal: Zirconium-oxide-doped lithium niobate,” *Appl. Phys. Lett.* **91**(8), 081908 (2007).
5. L. Wang, S. Liu, Y. Kong, S. Chen, Z. Huang, L. Wu, R. Rupp, and J. Xu, “Increased optical-damage resistance in tin-doped lithium niobate,” *Opt. Lett.* **35**(6), 883–885 (2010).
6. T. Volk and M. Wöhlecke, *Lithium Niobate Defects, Photorefractive and Ferroelectric Switching*, Springer Series in Material Science (Springer-Verlag, 2008), Vol. 115.
7. H. Liu, Q. Liang, M. Zhu, W. Li, S. Liu, L. Zhang, S. Chen, Y. Kong, and J. Xu, “An excellent crystal for high resistance against optical damage in visible-UV range: near-stoichiometric zirconium-doped lithium niobate,” *Opt. Express* **19**(3), 1743–1748 (2011).
8. F. Abdi, M. Aillerie, M. Fontana, P. Bourson, T. Volk, B. Maximov, S. Sulyanov, N. Rubina, and M. Wöhlecke, “Influence of Zn doping on electrooptical properties and structure parameters of lithium niobate crystals,” *Appl. Phys. B* **68**(5), 795–799 (1999).
9. F. Rossella, D. Grando, P. Galinetta, V. Degiorgio, and E. Kokanyan, “Photoconductive and electro-optical properties of Hf doped lithium niobate crystals,” *Ferroelectrics* **352**, 143–147 (2007).

10. M. Abarkan, M. A. Aillerie, J. P. Salvestrini, M. D. Fontana, and E. P. Kokanyan, "Electro-optic and dielectric properties of Hafnium-doped congruent lithium niobate crystals," *Appl. Phys. B* **92**(4), 603–608 (2008).
11. N. Argiolas, M. Bazzan, M. V. Ciampolillo, P. Pozzobon, C. Sada, L. Saoner, A. M. Zaltron, L. Bacci, P. Minzioni, G. Nava, J. Parravicini, W. Yan, I. Cristiani, and V. Degiorgio, "Structural and optical properties of zirconium doped lithium niobate crystals," *J. Appl. Phys.* **108**(9), 093508 (2010).
12. V. G. Plotnichenko, V. O. Nazaryants, E. B. Kryukova, and E. M. Dianov, "Spectral dependence of the refractive index of single-crystalline GaAs for optical applications," *J. Phys. D Appl. Phys.* **43**(10), 105402 (2010).
13. P. Minzioni, G. Nava, I. Cristiani, W. Yan, and V. Degiorgio, "Wide-band measurement of refractive index and birefringence in lithium niobate crystals with different Li content" (unpublished).
14. P. Minzioni, I. Cristiani, V. Degiorgio, and E. P. Kokanyan, "Strongly sublinear growth of the photorefractive effect for increasing pump intensities in doped lithium-niobate crystals," *J. Appl. Phys.* **101**(11), 116105 (2007).
15. L. Solymar, D. J. Webb, and A. Grunnet-Jepsen, *The Physics and Application of Photorefractive Materials* (Clarendon Press, 1996).
16. M. Abarkan, J. P. Salvestrini, M. D. Fontana, and M. Aillerie, "Frequency and wavelength dependences of electro-optic coefficients in inorganic crystals," *Appl. Phys. B* **76**(7), 765–769 (2003).

1. Introduction

The synthetic crystal Lithium Niobate (LN) plays a key role in integrated optical devices for electro-optic (EO) signal modulation and frequency conversion. Unfortunately the insurgence of photorefractivity in such crystals, when illuminated by visible or near-infrared light, requires either high-temperature operation or the use of doped LN crystals. It is known that photorefractivity can be strongly reduced by employing stoichiometric LN or MgO-doped LN, but both approaches are not satisfactory because it is very difficult to grow crystals with high optical quality. Some recent papers have shown that the photorefractivity of congruent LN (cLN) can be strongly reduced by doping the crystal with a small amount of tetravalent ions, such as Hf [1–3], Zr [4] and Sn [5]. Since a key role in the photorefractive process is played by the presence, in the cLN crystal, of Li-sites occupied by Nb ions, the aim of doping is that of removing these native defects by incorporating the dopant ion at the Li-site [6]. It is customary to introduce the concept of a "threshold" concentration, corresponding to the minimum doping concentration required for the complete removal of Nb_{Li} defects. Above this concentration value the crystal photorefractivity is strongly suppressed. Several properties of the doped crystals present indeed, in correspondence of the threshold concentration, an abrupt slope-change in their dependence on dopant concentration, as shown in the case of Hf:LN by the behavior of the crystal birefringence and of the phase-matching wavelength for second-harmonic generation [3]. The interesting aspect is that, in the case of tetravalent ions, the concentration required to obtain a substantial reduction of photorefractivity should be much lower than the value of 5.5mol% found with divalent ions, such as Mg [6]. Generally speaking, lower dopant concentrations make easier the growth of large homogenous crystals. A very recent report indicates that even lower dopant concentrations can be used by considering near-stoichiometric zirconium-doped LN crystals [7], even if the growth of non-congruent crystals clearly adds some difficulty.

In this work we concentrate on Zirconium-doped congruent LN crystals (hereafter indicated as Zr:LN). We performed measurements of the refractive indices in a wide wavelength range as functions of Zr concentration, with the aim not only to assess the value of the threshold concentration, but also to collect data useful for the design of optical devices based on Zr:LN crystals. Moreover, in order to set the ground for the utilization of these crystals in EO and nonlinear optical devices, we investigated the dependence of crystal photorefractivity on the incident power, which is a very important aspect, little studied in the literature concerning LN crystals. Finally, as photorefractive-resistant impurities may affect the electro-optical (EO) properties of LN crystals, specific investigations were performed to evaluate the EO-coefficients as a function of dopant concentration. Similar studies reported in the literature showed that the EO coefficients of Zn:LN varied by several pm/V as a function of Zn concentration, following a sort of oscillating trend [8]; conversely, for Hf doping no significant dependence of the EO coefficients on the doping concentration was revealed within the experimental error [9,10]. The same behavior is expected also for Zr, in force of its similarity with Hf; however, to the best of our knowledge, there are no reports on the EO response of Zr:LN.

Our light-induced birefringence experiments lead to conclude that, for intensity levels as in nonlinear optical devices, the concentration of ZrO₂ needed to suppress photorefractivity is in the range 2.0-3.0 mol%, somewhat larger than the value of 2.0 mol% at which the kink in crystal linear birefringence is observed. On the other side, the EO response of over-threshold Zr:LN crystals is as large as in pure ones. The reported data confirm that Zr:LN is a very promising candidate for the realization of efficient all-optical nonlinear devices.

2. Experimental methods

The Zr:LN crystals were grown by the Czochralski technique and subsequently poled at high temperature, at the University of Padova. The samples were cut and polished so as to obtain rectangular prisms with optical grade facets. The principal axes are perpendicular to crystal facets, and the sample size is about 10 × 4 × 8 mm (X × Y × Z). Details about the growth method and the crystal characterization can be found in [11].

2.1 Refractive index measurement

The ordinary and extraordinary refractive indices, n_o and n_e , were measured at 23°C in a wide wavelength interval by the method of interference refractometry [12], which consists in illuminating with a broadband light source a thin parallel crystal plate and observing the transmission peaks in the output spectrum due to the Fabry-Perot effect. The used broadband light source is an incandescence lamp, emitting in the wavelength interval 400 - 1700 nm. The details of both the experimental procedure and numerical analysis used to determine crystal refractive indices, as well as birefringence, can be found in [13].

2.2 Photorefractivity measurement

We call Δn_o and Δn_e the photo-induced changes of the ordinary and the extraordinary index of refraction respectively. The light-induced birefringence change, $\delta\Delta n = \Delta n_e - \Delta n_o$, was measured by using the Sénarmont method [1,14]. The photorefractive effect was induced by a 532-nm laser beam, linearly polarized along the c -axis and propagating along the crystal y -axis, and probed by a He-Ne laser beam, with $\lambda = 632.8$ nm. By using a phase-sensitive scheme, the $\delta\Delta n$ detection sensitivity of 10^{-6} was achieved. Birefringence variations were measured at intensity levels varying from 155 W/cm² to 1800 W/cm². As the raw data contain, besides the contribution due to photorefractivity, a significant contribution coming from the temperature change of the crystal; repeated illumination cycles were applied to the crystals, making it possible to separate the thermal contribution from the photorefractive effect [1].

In order to investigate the photorefractive behavior at beam-intensities larger than those compatible with our Sénarmont-based experimental setup, we exploited the following qualitative approach [2]. The 532-nm laser beam was focused by means of a convex lens onto the 4-mm thick crystal sample placed in the focal plane and we observed the distortion of the spot produced, in the far-field, by the light beam transmitted through the crystal. In fact, when the laser intensity induces a significant photorefractive effect, the change of the crystal refractive indices produces a significant defocusing of the beam, so that beam smearing and elongation along the c -axis is observed.

2.3 Measurement of the electro-optic response

The EO response of the Zr:LN crystals was measured at $\lambda = 632.8$ nm, within the wide transparency region of the material. An AC electric field was applied along the c axis of the crystals through silver paint electrodes. The electric field frequency was 400 Hz, well below the piezoelectric resonance, leading to the constant stress EO coefficients. When a laser beam is launched into the crystal sample with the linear polarization at 45° with respect to the crystal c axis, the two components of the polarization accumulate an EO-induced mutual phase delay Γ_m given by Eq. (1), λ being the beam wavelength, L the optical path in the sample, d the electrode spacing, V_m the amplitude of the applied voltage, and $r_c = r_{33} - (n_o/n_e)^3 r_{13}$ the effective electro-optic coefficient.

$$\Gamma_m = \frac{2\pi}{\lambda} \left[\frac{1}{2} n_e^3 r_c \right] \frac{V_m}{d} L \quad (1)$$

A polarizer is set after the crystal, at -45° with respect to the crystal optical axis. The intensity of the light beam transmitted through the polarizer, I_{out} , depends on the total phase delay, including the phase delay originated via the natural birefringence and the EO phase delay Γ_m . According to the method outlined in [15], Γ_m can be measured by recording I_{out} as a function of the total phase delay. As Γ_m varies linearly with the applied voltage, the r_c coefficient was conveniently retrieved from the slope of the line interpolating the experimental Γ_m , measured at several voltage amplitudes, ranging from 10 to 110 V. The overall experimental uncertainty on the r_c values was estimated to be about 5%. Different regions of each sample were tested, and the spread of values of the EO coefficients was less than 5%, thus confirming the sample homogeneity.

3. Results and discussion

3.1 Refractive indices and birefringence

We present in Fig. 1 the measured behavior of both refractive indices as a function of λ for four LN crystals (one pure and three Zr-doped). When comparing measurements performed with samples from the same crystal boule, but with different thickness, the uncertainty on the refractive-indices is lower than ± 0.003 . It should be noted that the largest source of error in our experiment is the correct evaluation of samples thickness.

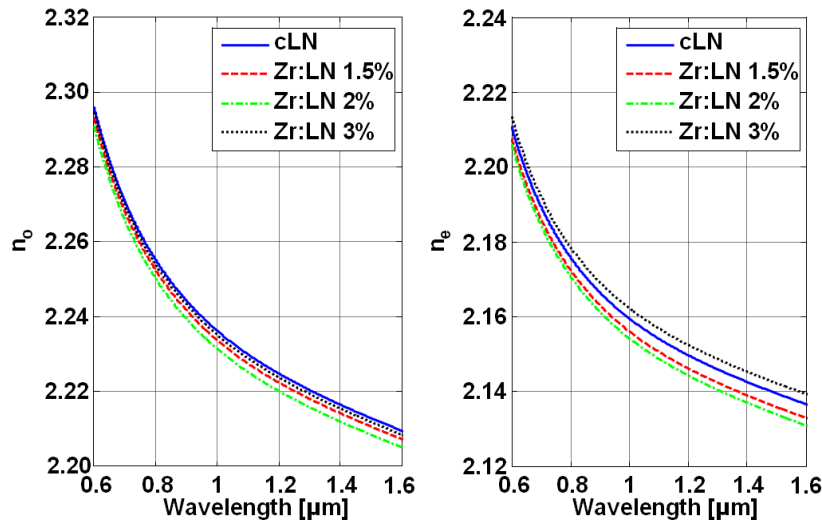


Fig. 1. n_o (left) and n_e (right) versus λ for different Zr concentrations in the melt. A significant increase of both refractive indices is observed when the crystal doped with 3.0 mol% is compared with the undoped one.

We report in Fig. 2 the dependence of n_o and n_e on ZrO_2 concentration at two specific wavelengths: 1550 nm and 1064 nm. We find that both n_o and n_e are slightly decreasing when the Zr content in the melt is increased from 0 to 2.0 mol%. Conversely, an increase of both indices, more marked for n_e , is observed when the dopant concentration is 3.0 mol%. It is interesting to note that the extraordinary refractive index of the 3.0mol% sample is larger than that of the congruent LN crystal.

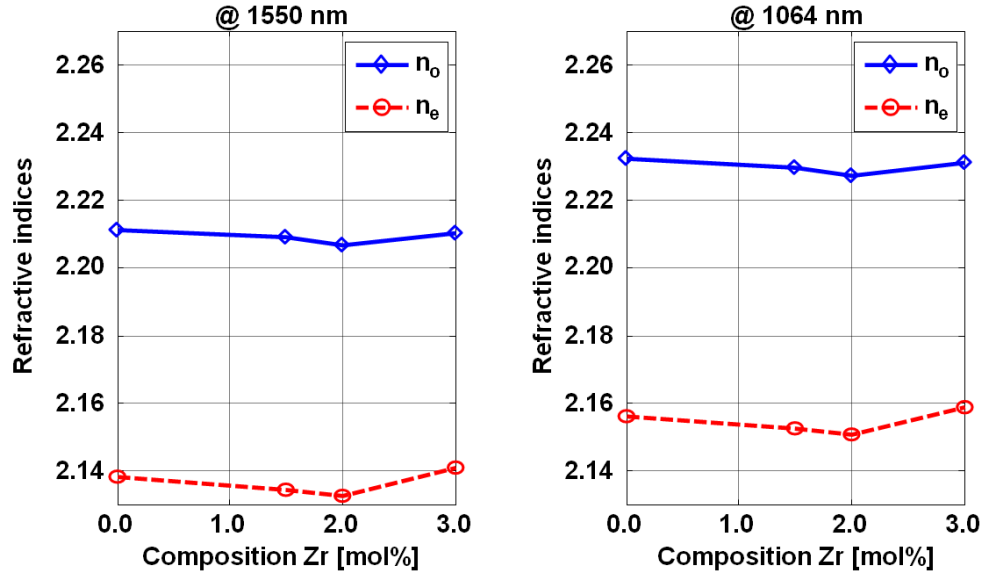


Fig. 2. Dependence of the refractive indices on the Zr content, at two different wavelengths.

Starting from the data in Fig. 2, we have also calculated the change of the crystal birefringence, Δn , as a function of the Zr concentration. Also in this case we estimate our relative error to be lower than $\pm 0.15\%$. The values of Δn relative to $\lambda = 1550 \text{ nm}$ are plotted in Fig. 3.

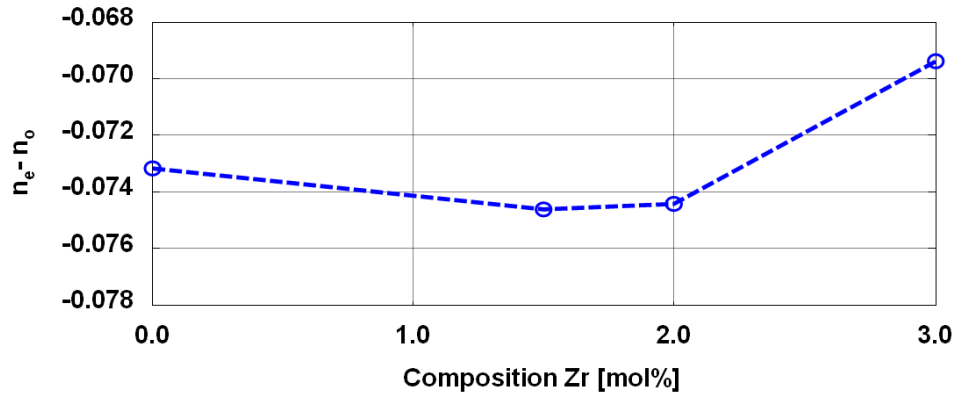


Fig. 3. Birefringence versus Zr content in the melt, calculated at the wavelength $\lambda = 1550 \text{ nm}$.

It should be noted that, although Fig. 3 looks very similar to Fig. 2 of [11], the numerical values of Δn are different. The reason is that the data analysis performed in this work takes fully into account the optical dispersion of the Zr:LN crystals, whereas in [11] we used a simplified analysis aimed at finding the value of the Zr concentration corresponding to the kink, without having the aim to give the absolute value of Δn .

3.2 Photorefractivity

The measured birefringence variation due to the photorefractive effect is shown in Fig. 4, for undoped cLN and some doped Zr:LN crystals. The left part shows, for four different values of the pump-beam intensity, the measured birefringence variation ($\delta\Delta n$) as a function of the dopant concentration. The plot clearly suggests the existence of a threshold concentration, at

about 2.0 mol%. A different visualization is proposed in the right part of Fig. 4, where the logarithm of $\delta\Delta n$ is plotted as a function of the logarithm of the pump beam intensity (expressed in W/cm^2), and the lines show a linear interpolation. It can be easily seen that for crystals with a dopant concentration above 2.0 mol%, the amount of induced damage is much smaller than that for pure cLN. Moreover the slope of the interpolating line corresponding to the 3.0 mol% crystal is significantly lower than that of the undoped crystal (≈ 0.6 for Zr 3.0 mol% and ≈ 1 for undoped sample), thus indicating a smaller sensitivity of photorefractivity to the beam intensity, as previously demonstrated in the case of Hf-doped LN crystals [14].

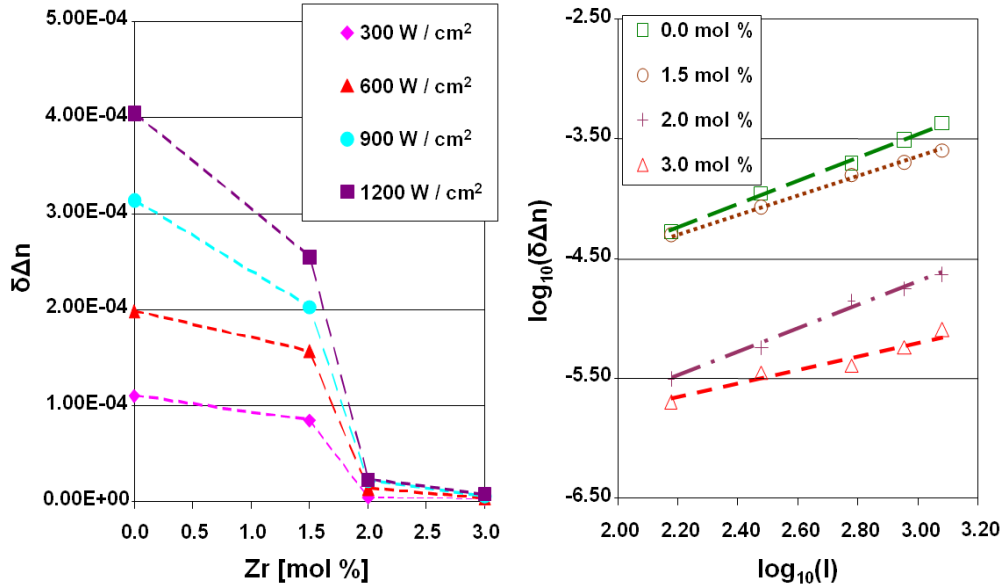


Fig. 4. Birefringence variation induced on Zr-doped LN crystals by the photorefractive effect. Left: $\delta\Delta n$ as a function of the ZrO_2 concentration in the melt. Each dashed line corresponds to a fixed value of the pump-beam intensity. Right: the $\delta\Delta n$ value is plotted as a function of the pump-beam intensity (measured in W/cm^2) on a Log-Log scale to highlight the different impact of intensity on pure and doped samples.

In order to demonstrate the behavior of doped crystals at larger beam intensities, we show in Fig. 5 the transmitted light spots obtained irradiating the samples with a laser power density of $7 \text{ kW}/\text{cm}^2$ for a few minutes. The images were recorded in the far-field, about 1 m away from the beam focus, and then rendered using a color-map, indicating in blue the low-intensity regions, and in red those with higher beam-intensity. We see that the 3.0 mol% Zr:LN crystal can withstand such a large intensity without noticeable beam smearing, whereas the beam propagating in the 2.0 mol% sample still presents some distortion, even if on a much smaller scale than that observed in the undoped sample, thus indicating that the threshold value given by the data in Figs. 2–4 should be somewhat exceeded in order to completely suppress photorefractivity.

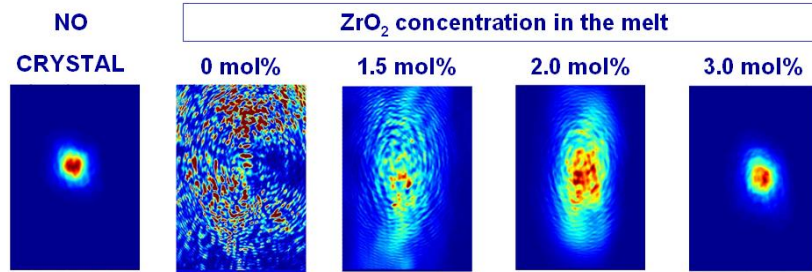


Fig. 5. Beam distortion observed in the far-field when a pump beam of intensity 7 kW/cm^2 is sent on the different crystals.

3.3 Electro-optic response

The measured constant-stress r_c coefficient is reported in Fig. 6 versus the concentration of ZrO_2 in the melt. The r_c coefficient appears to be very slightly influenced by Zr doping, consistently with the behaviour observed in Hf:LN crystals [9,10].

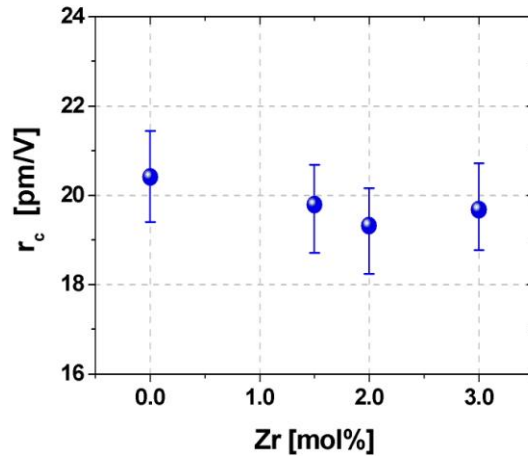


Fig. 6. Effective EO coefficient of Zr:LN as a function of Zr concentration ($\lambda = 632.8 \text{ nm}$, AC electric field frequency = 400 Hz).

The minimum value of the EO coefficient was measured to be 19.2 pm/V in the case of the 2.0 mol% Zr doped sample. It could suggest the existence of a doping-induced lattice reorganization, in coincidence with the above mentioned photorefractive concentration threshold. However no firm conclusion can be derived because of the overlapping error-bars. It should be noted that the piezoelectric contribution to the constant stress effective EO coefficient is below our experimental uncertainty [16], so that the reported EO coefficient values are expected to hold even when high frequency electric fields are applied, as in EO modulators for optical communication systems.

4. Conclusion

The presented results offer a complete characterization of Zr:LN crystals in view of their exploitation as substrates for low photorefractivity wavelength conversion devices.

The low-intensity and high-intensity data, presented in Fig. 4 and Fig. 5 respectively, show that the doping concentration of Zr:LN crystals to be used in a photorefractivity-free device should be somewhat larger than 2.0 mol%. It is worth noting that the theoretical threshold

concentration of dopant, measured inside the crystal, should correspond to the minimum concentration needed to remove all Nb_{Li} defects [6].

The constant stress EO response of Zr:LN was investigated within the wide transparency window of the material and the effective EO coefficient r_c resulted to be fairly comparable with that of pure congruent LN. This result demonstrates that Zr doping, besides being efficient for suppressing the photorefractive optical damage, does not negatively affect the EO response of LN crystal, one of the most relevant functional properties of LN.

Considering that the growth of good quality Zr:LN crystals, doped above threshold, should be easier than for Mg:LN, the overall scenario presented in this work and in [4], [7], and [11], clearly indicates that Zr-doped LN could represent the optimal choice for the realization of room-temperature devices, such as EO-modulators and all-optical wavelength converters. Moreover the refractive-indices results suggest that, similarly to Titanium indiffusion, it will probably be possible to fabricate low-photorefractivity optical waveguides by local Zr-indiffusion, without going through the step of growing doped LN crystals.

Acknowledgments

This work has been supported by Fondazione CARIPLO (Rif. 2007.5193) and by the Fondazione Ca.Ri.Pa.Ro (Fondazione Cassa di Risparmio di Padova e Rovigo, Italia) by financing the Excellence Project 2008-2009 “Integrated visible frequency converter based on doped periodically poled lithium niobate crystals with enhanced optical damage resistance”.